ISOTOPIC FISSION FRAGMENT DISTRIBUTIONS IN THE THORIUM REGION PRODUCED IN INVERSE-KINEMATICS WITH a ^{232}Th BEAM*

A. Cobo[a,b], L. Bégué-Guillou[a,b], D. Ramos[a], A. Lemasson[a]
M. Rejmund[a], P. Morfouace[c], M. Caamaño[d], J. Frankland[a]
J. Taieb[c], I. Jangid[a], A. Francheteau[a], T. Tanaka[a], B. Mauss[c]
C. Schmitt[e], N. Kumar[e], E. Clement[a], G. de France[a], A. Navin[a]
J.A. Dueñas[f], F. Angelini[g,h], C. Ciampi[a], B. Errandonea[d]
B. Jacquot[a], M. Lalande[a], M. Lozano[d]
J.L. Rodríguez-Sánchez[i], L. de Arruda[a,b,j], I. Tsekhanovich[k]
D. Gruyer[l], L. Audouin[m], H. Sengar[a], S. Kumar[a]

[a]GANIL, CEA/DRF — CNRS/IN2P3
Bd Henri Becquerel, BP 55027, 14076 Caen Cedex 5, France
[b]Université de Caen-Normandie, Normandie Université, 14000 Caen, France
[c]CEA, DAM, DIF, 91297 Arpajon, France
[d]Universidade de Santiago de Compostela, 15706 Santiago de Compostela, Spain
[e]Institut Pluridisciplinaire Hubert Curien, CNRS/IN2P3-UDS
67037 Strasbourg Cedex 2, France
[f]Departamento de Ingeniería Eléctrica y Centro de Estudios Avanzados en Física, Matemáticas y Computación, Universidad de Huelva, 21007 Huelva, Spain
[g]INFN LNL Legnaro, viale dell'Università 2, 35020 Legnaro (Padova), Italy
[h]Università di Padova and INFN Sezione di Padova, Padova, Italy
[i]CITENI, Campus Industrial de Ferrol, Universidad de la Coruña, 15403 Ferrol, Spain
[j]Department of Physics and Astronomy, Uppsala University
Box 516, 75120 Uppsala, Sweden
[k]CENBG, CNRS/IN2P3-Université de Bordeaux, 33170 Gradignan, France
[l]LPC Caen, France
[m]Université Paris-Saclay, CNRS, IJC Lab, 91406 Orsay, France

Received 13 December 2024, accepted 19 December 2024,
published online 10 April 2025

This work presents the preliminary fragment distributions produced through transfer-induced fission with a ^{232}Th beam, which has been accelerated for the first time at GANIL on a ^{12}C target. The experimental setup is described, as well as a newly implemented technique based on Machine Learning aiming at improving the resolution. The fragment mass and charge distributions for fission of ^{244}Cm and ^{234}U at different excitation energies are shown to illustrate the capability of the setup and quality of the results.

DOI:10.5506/APhysPolBSupp.18.2-A12

* Presented at the 57$^{\text{th}}$ Zakopane Conference on Nuclear Physics, *Extremes of the Nuclear Landscape*, Zakopane, Poland, 25 August–1 September, 2024.

1. Introduction

After the discovery of fission in 1939, the first theoretical model described this phenomenon as a competition between the repulsive Coulomb interaction and the attractive nuclear forces, making a liquid drop (LD) vary its shape through time [1]. If one considers such a macroscopic model, only a symmetric fission mode would be expected. However, since the early measurements, the asymmetric fission has been observed; where the final system is composed of a heavier and a lighter fragment. In order to fully understand these observations, theoretical calculations need to include microscopic features in the liquid drop model, like shell structure; and involve different deformation parameters namely quadrupole and octupole deformations [2].

In order to constrain the models, measurements are centred around correlations between the different observables on either the entrance channel (the one concerning the fissioning system) or/and the exit channel (related to the fission fragments and their de-excitation). In the beginning, mainly the total kinetic energy and the mass of the fission fragments were obtained. When the inverse-kinematics technique was introduced, the atomic number of the fission fragments could be measured [3]. This was possible due to the kinematic boost given by the heavier beam, which increases the kinetic energy of the fission fragments and allows for the distinction between different elements through the ΔE–E method, for example. This technique was introduced at GANIL through the VAMOS++ spectrometer, which permits the isotopic identification of the fragments thanks to the trajectory reconstruction [4].

After performing numerous studies with an ^{238}U beam and various targets [5], a new beam was used for the present experiment: ^{232}Th. This beam became available at GANIL in 2024, and it was first accelerated at Coulomb energies on a ^{12}C target. This combination allowed us to populate several fissioning systems through transfer reactions, such as ^{234}U or ^{230}Th, among others. Thanks to this, it was possible to access an actinide region closer to the known transition between symmetric and asymmetric fission [6]. Additionally, the fissioning systems produced in this experiment allowed us to study the shell closure at octupole deformation [7, 8] and its evolution along the actinides.

2. Experimental setup

A beam of ^{232}Th^{30+} was accelerated for the first time at GANIL and transported to a ^{12}C target at an energy of 6.06 MeV/A, and an intensity of ~ 1 pn$A$. The used detection system is shown in figure 1, and it can be divided into two categories: target position (inside the blue/black rectangle) and focal plane detectors.

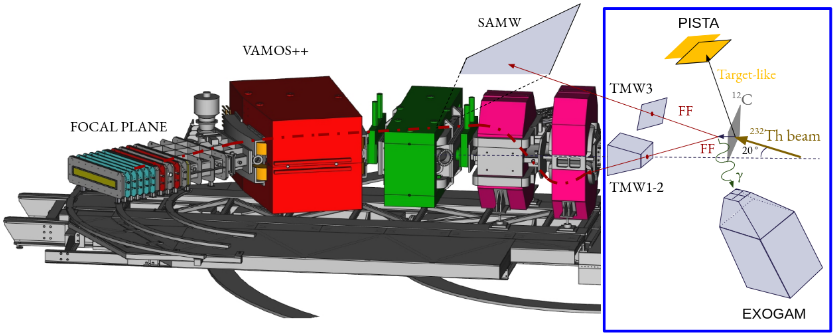

Fig. 1. (Colour on-line) Experimental setup of the VAMOS++ spectrometer. The blue/black rectangle indicates the detectors in the target area.

2.1. Target position detectors

As the name suggests, these detectors were placed around the Carbon target. On the one hand, PISTA (Particle Identification Silicon Telescope Array) was introduced in order to measure the energy and angle of the target-like ejectiles. This detector replaced the earlier used Si telescope (SPIDER) [9]. The new highly striped silicon detector consists of 8 trapezoidal, 100 μm thick, horizontally striped ΔE detectors, followed by other 8 trapezoidal, 1 mm thick, vertically striped E detectors. This combination enables the isotopic identification of the carbon-like particle, emitted after the multi-nucleon transfer reaction; as well as the determination of its linear momentum vector. Assuming a binary reaction, one can determine the fissioning system and its excitation energy [9].

On the other hand, the VAMOS++ spectrometer was placed at 20° with respect to the beam direction to detect one of the fragments emitted in the fission. A pair of Dual Position Sensitive Multi-Wire Proportional Counter (DPS-MWPC) detectors (labelled TMW1-2), with dimensions of 40×61 mm^2 and 65×93 mm^2, were placed in front of its entrance. These detectors were designed to operate at low pressure (6 mbar of isobutane in this case), being able to determine the X and Y positions, and to provide a fast time signal for every fission fragment before entering the VAMOS++ spectrometer [10]. This information is used to determine the velocity vector of a given fission fragment. Even though other detectors were present in the target position, they will not be presented here.

2.2. Focal plane detectors

In order to identify the atomic number of the nuclei, a highly segmented Ionization Chamber (IC) was located at the end of the particle trajectory, filled with CF_4 gas at a pressure of 100 mbar (figure 2). Three different segment sizes are present in the ionization chamber: 4 sections of 3 cm (0–3), 2 sections of 6 cm (4–5), and 4 last sections with a total length of 12 cm each (6–9). This feature permits to perform numerous ΔE–E combinations, thus improving the detector resolution for extracting the Z number.

For the mass identification, another pair of DPS-MWPCs (labelled FPMW0-1) was placed before the IC (figure 2). In this case, each detector was 1 m large in the dispersive axis of VAMOS (X) and 16 cm long in the perpendicular axis (Y). Both detectors were placed in a common 6 mbar isobutane gas volume separated by 17.75 cm and surrounded by two Mylar windows (0.6 μm and 2.4 μm thick). A total of 992 vertical wires (X position) and 160 horizontal wires (Y position) provide the position of the fission fragment at each Multi-Wire. In addition, the central cathode was divided into 20 segments (known as Multi-Wire number) in order to reduce the capacitance, providing a time signal every 5 cm. The combination of two X or Y values can be used to extract the polar and azimuthal angles (θ and ϕ).

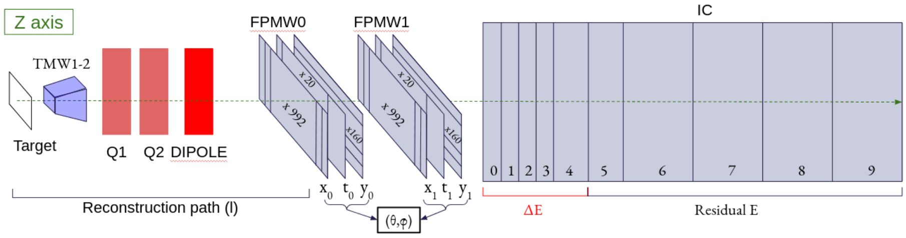

Fig. 2. The set of detectors used for the fission-fragment identification of VAMOS++ spectrometer. The different IC sections are depicted alongside the number of wires in the Focal Plane Multi-Wire detectors (FPMW).

3. VAMOS++ identification

One of the biggest strengths of VAMOS++ is its mass resolution, due to its feature of being able to reconstruct the particles' magnetic rigidity ($B\rho$). The idea is to extract the fragment hit positions of both Focal Plane (FP) detectors (x_0 and x_1) and the relatives angles, to obtain the $B\rho$ and Flight Path (l) of the given fission fragment using the reconstruction of its trajectory through the spectrometer [11]. These parameters, combined with the Time-of-Flight (ToF), are used to extract the mass-over-charge ratio of the fission fragment. The ToF was computed with the time signals of the first FPMW and first TMW, which are separated by 7.741 m

$$B\rho = \frac{p}{q} = \frac{\gamma m v}{q} = \frac{\gamma (A m_u)(\beta c)}{eQ} = 3.107 \times \frac{A}{Q} \times \beta\gamma\,, \tag{3.1}$$

where A indicates the mass number, Q the charge state, γ the Lorentz factor, and β the velocity relative to the speed of light.

This indicates that the position resolution of the Multi-Wires will ultimately have a strong impact on the mass resolution. Therefore, new methods to improve the position reconstruction can be very useful.

3.1. Machine Learning technique to improve the position resolution

Due to the design of the DPS-MWPC, every time a nucleus passes through the gas, a signal is generated in several position wires (figure 3 (a)). This permits to have a higher position resolution than the wire separation, using the mean of the distribution. During the past years, a hyperbolic secant (S) fit has been performed to the charge distribution; as it has been proven to have a better performance than the weighted average method (WA) [12].

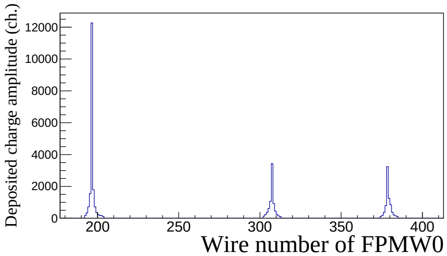

(a)

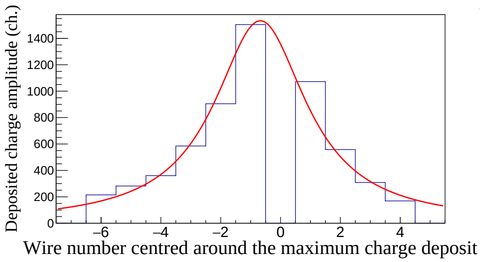

(b)

Fig. 3. (a) Charge distributions of three different fission events impinging on FPMW0. (b) A Lorentzian fit performed to a charge distribution from (a), removing the maximum amplitude peak.

In principle, with the proper calibration of the wires, the S-method should not give any problem. However, during this experiment, a significant amount of charge distributions presented a maximum value higher than the expected one, even reaching saturation for some events. This feature made the fitted position value biased by a specific wire, diminishing the resolution capability of the detection system. To restore the resolution of the MWPCs, the wire corresponding to the maximum charge amplitude must be removed before performing the fit, as depicted in figure 3 (b). The main drawback of this technique is that one needs to perform the fit on an event-by-event basis, for each of the FPMWs. This is not only memory-consuming, but it significantly slows down the computation process. Here is where the Machine Learning method enters into play.

For this task, the ROOT library TMultiLayerPerceptron(T-MLP) [13] was employed. For the input nodes, the charge amplitudes of the 4 wires located at the left and right of the maximum charge were chosen; having a total of 8 data points to represent the distribution. To generalize, all the distributions were centred around the maximum amplitude wire. The designed architecture had a first hidden layer with 5 nodes, a second hidden layer with 3 nodes, and an output neuron — corresponding to the mean. In the training phase, this mean was obtained by performing the Lorentzian fit of the charge distribution without the maximum charge peak, as shown in figure 3 (b).

As it can be seen in figure 4 (a), the maximum-less Lorentzian fit removes the pixelization on the angle. Regarding the reconstructed A/Q, a worsening in θ_f resolution has a larger impact at larger MW numbers (figure 4 (b)); agreeing with what is stated in [11]. The observed reconstruction performed with the neural network appears to correct this effect, improving the detector resolution. On top of that, this method reduces the execution time by a factor of 4 compared to the standard fitting procedure; and it also enables to use of up to 10% more events than the hyperbolic secant method, as it is less sensitive to the missing wires.

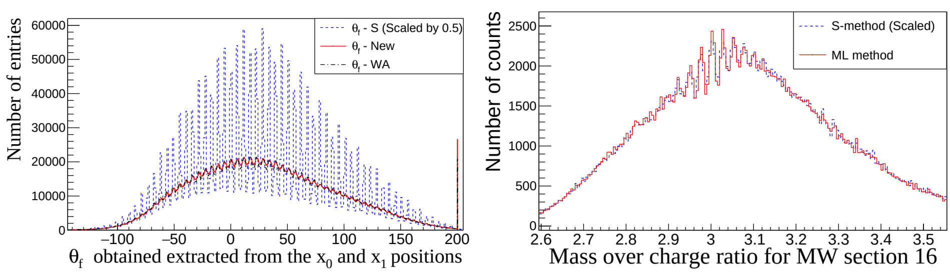

(a) (b)

Fig. 4. (Colour on-line) (a) Comparison of the θ_f angle obtained between the hyperbolic secant (blue/grey dashed), weighted average (black dot-dashed), and Machine Learning (red/light grey solid) methods. (b) Comparison of the A/Q computed for the Multi-Wire section number 16, between the hyperbolic secant method (blue/black dashed) and the ML method (red/grey solid).

3.2. Mass, charge state, and atomic number reconstruction

Once the A/Q is obtained, the different charge states of the fragments need to be computed to properly retrieve its mass. To begin with, the kinetic energy of the fragment is calculated as a weighted sum of the charge deposited in the different IC sections (IC_i), which can be converted into mass using Einstein's relation

$$E = \sum_{i=0}^{9} a_i \times \mathrm{IC}_i \rightarrow A_{\mathrm{IC}} = \frac{E}{931.494(\gamma - 1)} \Rightarrow Q = (M_{\mathrm{IC}}/(A/Q)) \ . \quad (3.2)$$

Then, knowing that the Q needs to have an integer value, the charge states are computed with the A/Q resolution; which is better than the initial IC resolution. Lastly, the mass of the fission fragment is recovered

$$Q_{\rm int} = \lfloor (M_{\rm IC}/(A/Q) + 0.5) \rfloor \Rightarrow A = Q_{\rm int} \times \frac{A}{Q} \,. \tag{3.3}$$

Concerning the Z value, the charge deposited in the first 5 sections of the IC was used as the ΔE, whereas the remaining 5 sections constituted the residual energy (see figure 2).

4. Preliminary results

Some preliminary results from the ongoing analysis are presented here. Figure 5 (a) is a clear indication of the capabilities of the new PISTA detector. The figure shows the isotopic separation of different target-like nuclei, which enables a proper distinction between different fissioning systems. By choosing two different systems (^{244}Cm and ^{234}U), it is possible to observe the evolution between a more symmetric fission into a highly asymmetric one, as depicted in figure 5 (b) in terms of the mass distribution of the fission fragments. This occurs not only due to the different properties between

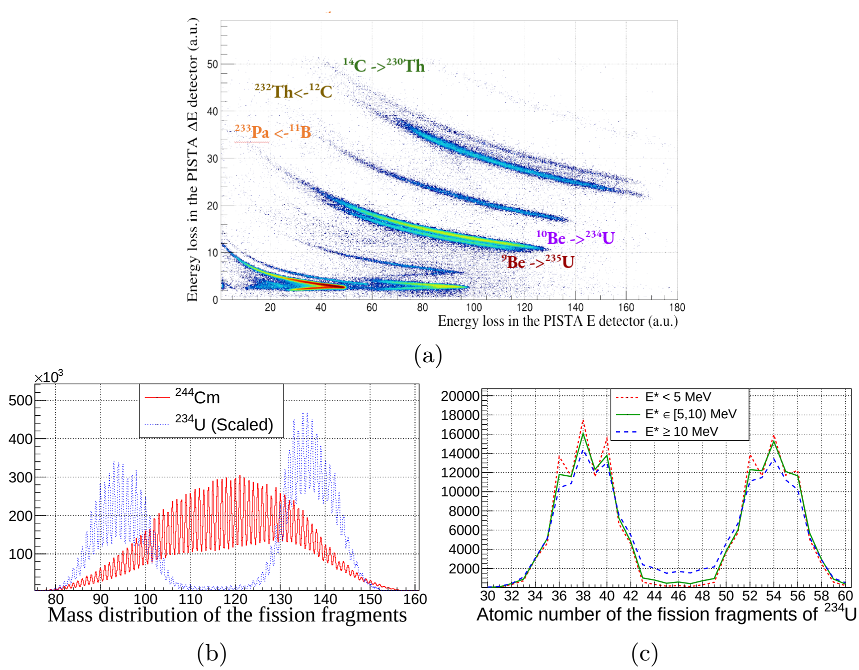

Fig. 5. (Colour on-line) (a) ΔE–E relation obtained with the PISTA detector, showing the PID capability. (b) Mass distribution of the fission fragments for ^{244}Cm (red/grey solid) and ^{234}U (blue/black dotted). The selection of the fissioning system has been obtained using the PISTA detector. (c) Atomic number distribution of the fission fragments for low (red/light grey dotted), medium (green/grey solid), and high (blue/black dashed) excitation energy of ^{234}U.

both mother nuclei, but it is primarily due to the higher excitation energy of the fissioning system formed in fusion, compared to the one in transfer.

Furthermore, by gating on the fissioning system excitation energy (E^*) reconstructed from the PISTA observables, the fragment properties can also be obtained as a function of excitation energy. This is shown in figure 5 (c), which presents the Z distribution for the fission of ^{234}U at three E^*. The distribution reveals a clear even–odd staggering effect (the even-Z elements are produced more than the odd ones), which is a known indication of the pairing effect. It is observed that this correlation decreases with the increase of the excitation energy of the system, as there is more intrinsic energy available to break the pairs. Lastly, an increase of production in the symmetric region is evidenced for higher E^*, another sign of the vanishing of shell effects.

5. Conclusions

We have shown the preliminary results of a recent experiment, mainly the fission fragment distributions obtained with a ^{232}Th beam impinging on a ^{12}C target. We have also introduced a new technique to improve the mass resolution based on Machine Learning. This method is still under development and is expected to further improve the resolution when applied to all the DPS-MWPCs present in the detection system. Finally, the great capabilities of PISTA are demonstrated, which, combined with the high resolution of VAMOS, offer a great setup for addressing open questions in the understanding of the fission process.

REFERENCES

[1] N. Bohr, J.A. Wheeler, *Phys. Rev.* **56**, 426 (1939).

[2] N. Schunck, L. Robledo, *Rep. Prog. Phys.* **79**, 116301 (2016).

[3] K.-H. Schmidt *et al.*, *Nucl. Phys. A* **665**, 221 (2000).

[4] M. Rejmund *et al.*, *Nucl. Instrum. Methods Phys. Res. A* **646**, 184 (2011).

[5] D. Ramos *et al.*, *Phys. Rev. C* **97**, 054612 (2018).

[6] P. Möller, J. Randrup, *Phys. Rev. C* **91**, 044316 (2015).

[7] G. Scamps, C. Simenel, *Phys. Rev. C* **100**, 041602 (2019).

[8] G. Scamps, C. Simenel, *Nature* **564**, 382 (2018).

[9] C. Rodríguez-Tajes *et al.*, *Phys. Rev. C* **89**, 024614 (2014).

[10] M. Vandebrouck *et al.*, *Nucl. Instrum. Methods Phys. Res. A* **812**, 112 (2016).

[11] A. Lemasson, M. Rejmund, *Nucl. Instrum. Methods Phys. Res. A* **1054**, 168407 (2023).

[12] K. Lau, J. Pyrlik, *Nucl. Instrum. Methods Phys. Res. A* **366**, 298 (1995).

[13] C. Delaere, «class TMultiLayerPerceptron», 2003, https://root.cern.ch/root/html516/TMultiLayerPerceptron.html